Molecular Vision 2008; 14:81-9 <http://www.molvis.org/molvis/v14/a10/>
Received 2 August 2007 | Accepted 12 December 2007 | Published 16 January 2008

©2008 Molecular Vision

Formation of amyloid fibrils in vitro by human γD-crystallin and its isolated domains

Katerina Papanikolopoulou,[1] Ishara Mills-Henry,[2] Shannon L. Thol,2 Yongting Wang,[2] Abby A.R. Gross,[3] Daniel A. Kirschner,[3] Sean M. Decatur,[4] Jonathan King[2]

[1]Department of Materials Science and Technology, University of Crete, Heraklion, Crete, Greece; [2]Massachusetts Institute of Technology, Department of Biology, Cambridge, MA; [3]Boston College, Biology Department, Boston, MA; [4]Mount Holyoke College, Department of Chemistry, South Hadley, MA

Purpose: Amyloid fibrils are associated with a variety of human protein misfolding and protein deposition diseases. Previous studies have shown that bovine crystallins form amyloid fibers under denaturing conditions and amyloid fibers accumulate in the lens of mice carrying mutations in crystallin genes. Within differentiating lens fiber cells, crystallins may be exposed to low pH lysosome compartments. We have investigated whether human γD-crystallin forms amyloid fibrils in vitro, when exposed to low pH partially denaturing conditions.

Methods: Human γD-crystallin expressed and purified from E. coli, is stable and soluble at 37 °C, pH7, and refolds from the fully denatured state back to the native state under these conditions. Purified Human γD-crystallin as well as its isolated NH2- and COOH-terminal domains were incubated at acid pH and subsequently examined by transmission electron microscopy, absorption spectroscopy in the presence of Congo red, FTIR, and low-angle X-ray scattering.

Results: Incubation of the intact protein at 37 °C in 50 mM acetate buffer pH 3 at 50 mg/ml for 2 days, led to formation of a viscous, gel-like solution. Examination of negatively stained samples by transmission electron microscopy revealed linear, non-branching fibrils of variable lengths, with widths ranging from 15 to 35 nm. Incubation with the dye Congo red generated the spectral red shift associated with dye binding to amyloid. Low-angle X-ray scattering from samples showed clear meridional reflection at 4.7 Å and a more diffuse reflection on the equator between 10 and 11 Å which is the typical "cross-β" X-ray fiber diffraction pattern for amyloid fibers. FTIR was used to follow the evolution of the secondary structure of γD-crystallin with time during incubation of the protein at pH 3. The native protein displayed a major band at 1640 cm-1 that converted during incubation at 37 °C to a band at 1616 cm-1. An additional band at 1689 cm-1 also appeared with time. The presence of bands in the regions about 1620 cm-1 and about 1680 cm-1 has been attributed to the formation of intermolecular β-sheet structure that characterizes the fibrillar amyloid motif. The isolated NH2-terminal 1-82 and COOH-terminal 86-174 domains of HγD-crystallin also formed amyloid fibrils after incubation under the same conditions, but to a lesser extent than the full length.

Conclusions: HγD-crystallin, as well as its isolated NH2-terminal 1-82 and COOH-terminal 86-174 domains of HγD-crystallin formed amyloid fibrils upon incubation at acid pH. Investigations of early stages in cataract formation within the lens will be required to assess whether amyloid fibrils play a role in the initiation of cataract in vivo.

The development of strategies for preventing or retarding growth of cataracts, as alternatives to surgical removal of mature cataracts, is hindered by our limited understanding of the mechanisms of lens opacification [1,2].

The transparency of the lens is largely determined by the properties of crystallins, the family of ocular lens proteins that are essential for maintaining the proper refractive index gradient needed for the focus of light onto the retina [3]. The crystallins within the central nucleus of the lens have to remain in their native conformation for a lifetime since these lens fiber cells are post-mitotic and lose their biosynthetic machinery during the differentiation process. The crystallins are present at high concentrations (200-450 mg/ml) and arranged in a closely packed environment [4-6].

The βγ-crystallins are structural proteins of the lens while the α-crystallins possess molecular chaperone properties and are able to interact with unfolded proteins in response to stress and to prevent their aggregation [7-12]. Human γD-crystallin (HγD-Crys) is the third most abundantly expressed γ-crystallin in the lens and contains 173 amino acids [13,14]. X-ray crystallographic studies at 1.25 Å resolution showed that the monomeric protein adopts the characteristic fold of the βγ-crystallin superfamily [15]. The protein consists of two highly homologous domains, each composed of two β-sheet Greek key motifs. The NH2-terminal and COOH-terminal domains (N-td and C-td) are joined together by a six-amino acid linker sequence and interact through side chain contacts at the domain interface [16]. HγD-Crys possesses differential domain

Correspondence to: Jonathan King, Massachusetts Institute of Technology, Department of Biology, 31 Ames Street, Cambridge, MA, 02139-4307; Phone: (617) 253-4700; FAX: (617) 252-1843; email: jaking@mit.edu

Dr. Gross is now at the BSRC "Alexander Fleming", Institute of Molecular Biology and Genetics 34 Fleming Street, 16672 Vari, Greece. Dr. Thol is now at 158 University Village, Apt E, Ames, IA 50010. Dr. Mills-Henry is now at Harvard University, Biological Laboratories, Rm 2081, 16 Divinity Ave, Cambridge, MA 02138.

stability with the C-td being more stable than the N-td [17]. Equilibrium unfolding/refolding experiments at near-physiologic conditions (pH 7 at 37 °C) demonstrated that the protein refolds through the sequential structuring of its domains, with the C-td refolding first [17]. Domain interface residues subsequently nucleate the refolding of the N-td. Equilibrium unfolding/refolding experiments also revealed the presence of a partially folded intermediate probably containing the C-td in its native conformation and the N-td in its random state [18].

During cataract development, insoluble aggregates of all three classes of crystallins accumulate in the lens and lead to light scattering and loss of lens clarity [19]. Protein precipitation and aggregation might occur by changes of the properties of crystallins driven by point mutations or age-related post-translational modifications. There are several types of hereditary cataracts that have been linked to mutations of human crystallin genes [20-26]. For example in HγD-Crys single amino acid substitutions are associated with juvenile-onset cataracts, which may be mediated through spontaneous crystallization or disulfide cross-linked aggregation of the mutants [27,28]. Lens opacity in these cases is, therefore, associated with reduction in the solubility of the native state and the formation of solid state complexes [29,30].

For mature-onset cataract, the mechanisms of aggregation in the aging lens are unlikely to be the same as for the rare inherited juvenile-onset cataracts. The crystallins of aged and cataractous lenses present a variety of covalent changes including deamidation [31,32], oxidation of methionine and cysteine residues, backbone cleavage [32], and glycation [33]. The consequence of these modifications may be conformational changes that alter the crystallin stability, leading to their denaturation and aggregation. Mature-onset cataract could be considered as a conformational disorder [22,34] where protein deposition may be driven by the formation of a partially folded intermediate [35,36].

At least 20 human protein misfolding and protein deposition diseases are characterized by the accumulation in different tissues of amyloid fibrils. The different pathologies are believed to arise from a common mechanism [36,37]. In each case, there is a change in the conformation of a normally folded protein, which leads to the formation of a partially folded intermediate from which amyloid fibrils can be formed by auto assembly [38-40]. The destabilization of the protein can be produced by mutations or by the introduction of partially denaturing conditions [41]. Amyloid is defined by three features, namely its tinctorial affinity for the dye Congo red, its unbranched fibrillar appearance upon analysis by electron microscopy and its characteristic "cross-β" X-ray diffraction pattern [36,37,42]. The ability of polypeptide chains to form amyloid structures is not limited to the disease-associated proteins. Proteins that are not known to be amyloidogenic in vivo have been shown to undergo self-assembly into fibrils in vitro [43-49].

Experiments performed under denaturing conditions with wild-type bovine crystallins demonstrated that all three classes of proteins are able to form amyloid fibers [50]. In mice Sandilands and coworkers [52] have shown that mutant truncated forms of the γ-crystallins form inclusions containing filamentous material in the lens that bind Congo red. Furthermore the purified truncated protein formed amyloid fibrils in vitro [51]. In vitro filament-like formation has also been identified upon interaction between α-crystallin and βL-crystallin.

Previous studies of the unfolding/refolding pathway of HγD-Crys in guanidine hydrochloride at 37 °C and pH 7 revealed an in vitro aggregation pathway that proceeded via the formation of partially folded species [53]. The aggregates were ordered with filamentous appearance, as seen by atomic force microscopy and could bind bisANS. In the present studies we demonstrate that at low pH in vitro γD-crystallin and its isolated domains polymerize into fibrillar aggregates. Using a combination of Congo red binding, Fourier transform infrared spectroscopy, X-ray fiber diffraction and electron microscopy approaches we present direct evidence that the fibrils are amyloid in character.

METHODS

Protein expression and purification: The HγD-Crys, N-td and C-td coding sequences were cloned into the pQE.1 plasmid (Qiagen, Valencia, CA) that added an NH_2-terminal 6-His Tag to the proteins. Bacterial expression and purification of the recombinant proteins has been described in a previous paper [17]. Briefly, protein expression was induced at 37 °C by addition of IPTG. After cell lysis by sonication and removal of the insoluble material by centrifugation, the supernatant was loaded onto a Ni-NTA column. The purified proteins were stored at 4 °C in 10 mM ammonium acetate pH 7 buffer.

Fibril preparation: To generate fibril samples, the proteins were incubated at 37 °C in 50 mM acetate buffer pH 3 at 5 mg/ml for 2 days. In these conditions the soluble crystallin proteins aggregated and formed a gel that, as we show in the Results, consists of amyloid fibrils. Fibril formation can be induced at pH 3 using a protein concentration as low as 50 μg/ml.

Electron microscopy: Samples of the proteins incubated at 37 °C in 50 mM acetate buffer pH 3 at 5 mg/ml for 2 days, were diluted to 1 mg/ml and deposited onto glow-discharged carbon-coated, formvar-filmed copper grids. They were subsequently negatively stained with 1% uranyl acetate and viewed in a JEOL 1200 transmission electron microscope. The dimensions of the fibrils were obtained directly from the micrographs.

Congo red staining: Samples were tested for Congo red binding by the spectroscopic band-shift assay [54]. Fibrils were formed as for electron microscopy and diluted into 500 mM sodium phosphate buffer pH 7 at a 0.5 mg/ml final concentration. Twenty-five μl of a 100 μM freshly prepared stock solution of Congo red were added to 475 μl of protein solution and spectra were recorded from 400 to 600 nm. Absorption spectra of protein samples in the absence of the dye were also collected at the same wavelengths, to subtract the scattering contribution of the aggregates from the spectrum of the dye in their presence.

FTIR measurements: HgD-Crys was dialyzed against deuterated 50 mM sodium citrate buffer pH 3 at a concentration of 20 mg/ml. The sample was placed between two CaF2 windows separated by a 100 mm spacer and placed within a water-jacketed cell. Sample temperature was held at 37 °C via a circulating water bath. FTIR spectra were measured on a Bruker Vector-22 FTIR spectrometer Each spectrum consisted of an average of 512 scans recorded with 4 cm-1 resolution. Spectra were measured every 30 min for up to 20 h. A spectrum of the blank buffer (also recorded at 37 °C) and of water vapor were subtracted from the protein absorbance spectrum.

X-ray fiber diffraction: Each pre-incubated protein fiber sample was prepared for X-ray diffraction, using two different methods. For the first preparation, each protein solution at a concentration of 5 mg/ml was aspirated into a 0.7 mm diameter siliconized thin wall glass capillary tube. The capillary tubes were sealed at the narrow end by flame. The wide end of the capillary was sealed with wax through which a pinhole was punched using a hot needle. The peptide solution in the capillary tube (which stood vertically) was then allowed gradually to dry under ambient temperature and humidity until the formation of a small, uniform birefringent disk. For the second preparation, 5-8 µl of protein fiber sample were deposited between the ends of two glass rods and air-dried. These samples were loaded into glass capillaries to be examined by X-ray diffraction. Measurements at room temperature from the samples were conducted using the Oxford diffraction Xcalibur PX Ultra system (Oxford Diffraction Ltd., Concord,MA) located in the laboratory of Dr. A. Andrew Bohm (Department of Biochemistry, Tufts University, Boston, MA) [55]. The CuKα X-ray beam was generated using an Enhance Ultra, which is a sealed tube-based system incorporating confocal multilayer optics. The X-ray beam was monochromated and the Kβ component was removed by means of the double bounce within the confocal optics. The X-ray beam was focused to 0.3 mm x 0.3 mm (full-width at half-maximum width at detector position). A two-dimensional Onyx CCD detector (Oxford Diffraction Inc., Concord, MA) was placed 85 mm from the sample position, covering the scattering range of Bragg spacing 1.8 Å-54 Å. The sample-to-detector distance was calibrated by a spherical ylid crystal ($C_{10}H_{10}SO_4$) or a cubic alum crystal according to the information given by manufacturer. The active range of the detector was 165 mm, and the two dimensional image (1024 x 1024 pixels; in 2x2 bin-

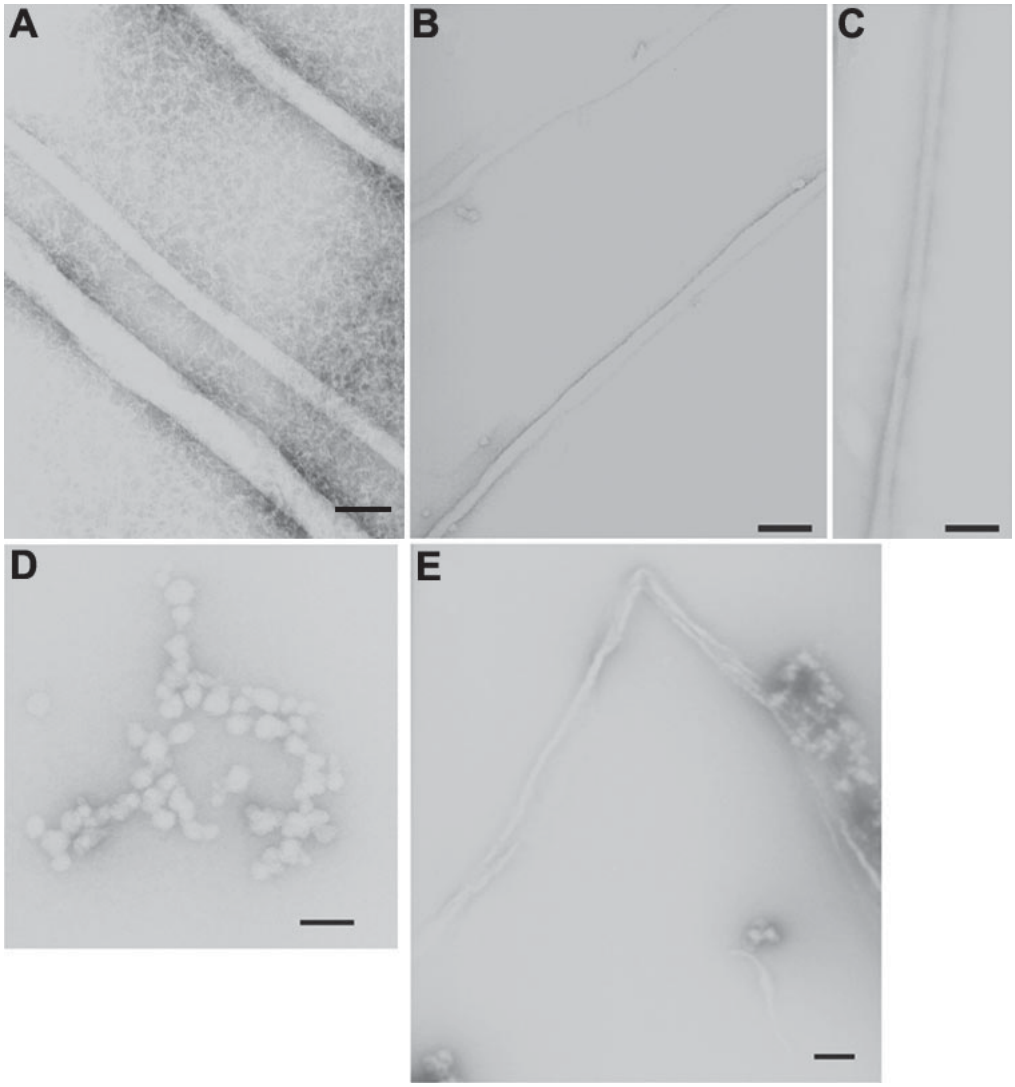

Figure 1. Electron micrographs of fibrils negatively stained with 1% uranyl acetate. Conditions were as follows: **A**: 5 mg/ml solution of the HγD-Crys into 50 mM acetate buffer pH 3 incubated at 37 °C for 2 days, **B**: 5 mg/ml solution of the HγD-Crys Ctd into 50 mM acetate buffer pH 3 incubated at 37 °C for 2 days, **C**: 5 mg/ml solution of the HγD-Crys Ntd into 50 mM acetate buffer pH 3 incubated at 37 °C for 2 days, **D**: 50 µg/ml solution of the HγD-Crys into 100 mM sodium citrate pH3 deposited on the grid after 2 h of incubation at 37 °C, **E**: 50 µg/ml solution of the HγD-Crys into 100 mM sodium citrate pH3 deposited on the grid after 6 h of incubation at 37 °C. The bar represents 1,000 Å.

ning) was collected using the software package CrysAlis (CrysAlis CCD and RED, version 171 [2004], Oxford, UK) and stored in the compressed image format IMG. Exposure time was 150-300 s. The diffraction image in the form of JPG as supplied by CrysAlis RED was translated to TIFF, and then displayed by NIH image software (developed at the USA National Institutes of Health). Using the known Bragg peaks of the fundamental period of 58.38 Å from silver behenate, the pixel size of the image was calculated as 121 μm for both the specimen to film distance of 85 mm.

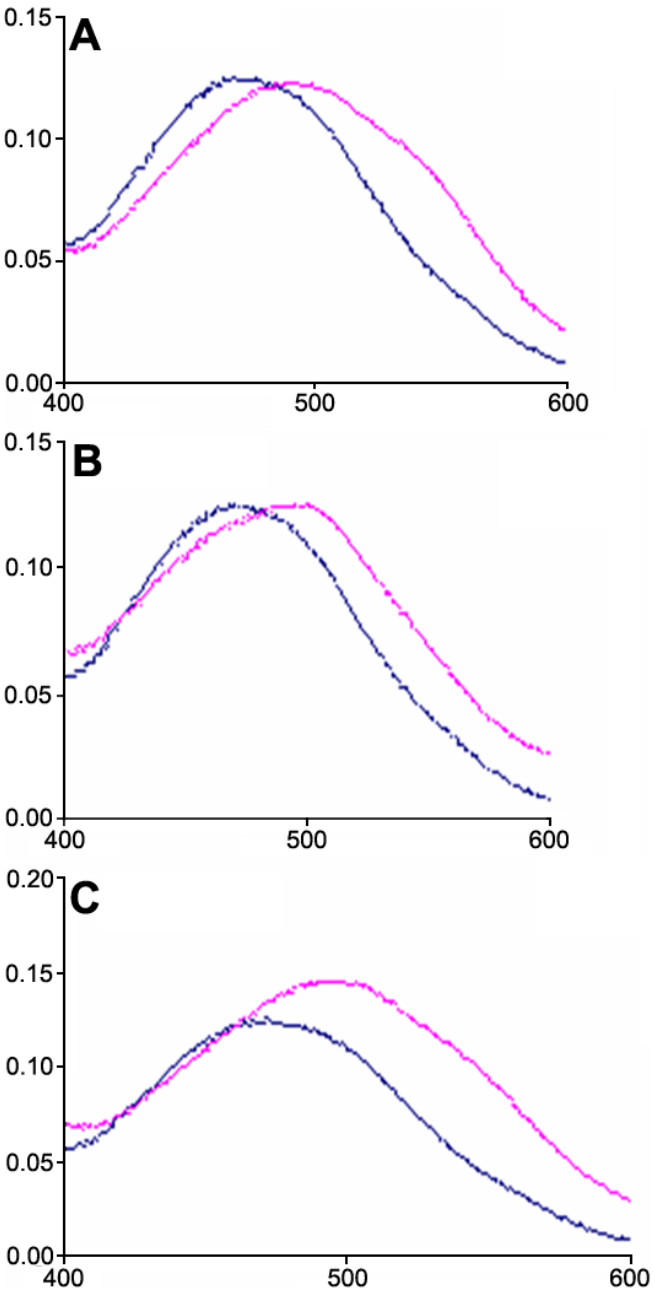

Figure 2. Congo red binding to crystallin fibrils. The spectra of 5 μM Congo red in the absence (blue line) and in the presence (red line) of fibrils formed by **A**: HγD-Crys, **B**: HγD-Crys Ctd, and **C**: HγD-Crys Ntd. Before adding the dye, the scattering of the peptide solutions was recorded and subtracted from the spectrum of the dye in their presence. Fibrils were formed by incubation of the proteins at 37 °C in 50 mM acetate buffer pH 3 at 5 mg/ml for 2 days and subsequently diluted in a 500 mM sodium phosphate buffer pH 7 at a 0.5 mg/ml concentration.

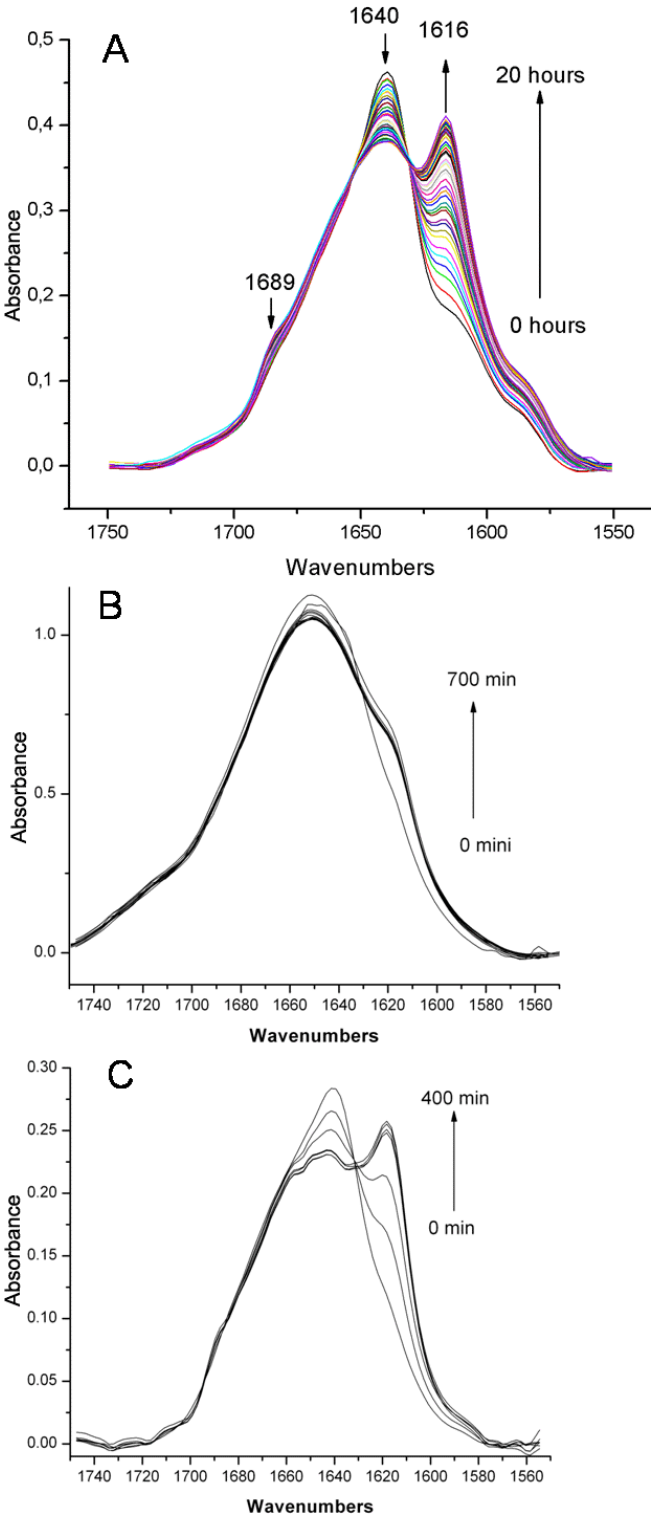

Figure 3. FTIR spectra as a function of incubation time from 0 to 20 h, at low pH, 37 °C. **A**: HγD-Crys, **B**: HγD-Crys Ctd, and **C**: HγD-Crys Ntd. The spectral shift associated with fibril formation is indicative of an increase in the extent of antiparallel β-sheet content.

RESULTS

Fibril formation as seen by electron microscopy: Complete wild type HγD-Crys as well as its N-td and C-td domains, were expressed and purified from E. coli strains. All three preparations were predominantly monomeric when characterized by liquid chromatography. On incubating the three crystallin proteins, namely HγD-Crys, HγD-Crys N-td and HγD-Crys C-td, at pH 3 and 37 °C, we observed the formation of a viscous, gel-like solution after a few hours. This conversion was associated with the presence of unbranched, long fibrils as revealed by electron microscopy of negatively stained samples. Figure 1A-C shows electron micrographs that were recorded after incubation of 5 mg/ml solutions for 2 days, for each of the three proteins. The fibrils display typical amyloid morphology. Their diameter ranged from 15 to 35 nm, similar to the width of fibrillar structures formed from other amyloidogenic proteins [39]. These results suggest that at pH 3 the proteins fail to remain correctly folded but instead they convert to insoluble fibrils through the disruption of their normal protein conformation.

The morphological development of the fibrils was better observed at protein concentrations as low as 50 μg/ml. The process of fibril formation started with small bead-like structures that have already been described in a variety of amyloidogenic systems [56-66]. After 6-8 h of incubation these prefibrillar aggregates could still be seen but in addition, structurally well defined species with fibrillar morphology began to appear. Figure 1D,E shows representative fields from grids where a drop of a 50 μg/ml HγD-Crys solution was deposited after 2 and 6 h of incubation in pH 3 at 37 °C. In high-concentration gel-like samples these oligomeric species were not present, suggesting their transformation to fibrils.

Congo red binding: Congo red is a diazo dye that interacts specifically with highly ordered cross β-sheet aggregates. Congo red birefringence is considered to be one of the three hallmarks of amyloid. The binding of the dye is revealed by the spectral difference between fibril-containing solutions and dye-only solution [54]. The absorbance maximum of the Congo red incubated in buffer alone increases and shifts to red upon interaction with ordered fibrils. Figure 2 shows the dye spectra in the presence of aggregates formed from HγD-Crys, HγD-Crys N-td, and HγD-Crys C-td. For the dye-binding assay the samples were diluted into pH 7 buffer, which did not solubilize the polymerized protein. The addition of the dye to samples containing crystallin fibrils produced the characteristic red-shift expected from interaction with amyloid fibrils.

Secondary structure of the peptides in their fibrillar state as determined by FTIR: FTIR is a key method for the study of the secondary structure of protein aggregates. Using this technique, we followed the structural transition of HγD-Crys with time during incubation of the protein in pH 3. The IR spectrum in the amide I' region of native HγD-Crys contains a single broad band, with maximum about 1638 cm-1, consistent with the spectra of other globular, β-sheet rich proteins. After incubation at pH 3, two new amide I' bands appear, at about 1616 and about 1689 cm-1. These bands are characteristic of the flat, extensive antiparallel β-sheets found in fibrous aggregates [67]. The transition from the native spectrum to the amyloid-type spectrum was monitored by collection of spectra at various time points, after shift to acid pH. The transition has a clear isosbestic point (Figure 3A).

The isolated, native N-td and C-td domain had similar IR spectra as the full length HγD-Crys. When incubated at pH 3, the IR spectra of both of these domains also developed new amide I' bands at 1616 cm-1 and 1689 cm-1, though to a smaller extent than seen in the full length HγD-Crys (Figure 3B,C).

X-ray fiber diffraction: Fibrils produced in acidic conditions were also examined by X-ray fiber diffraction. The recorded diffraction patterns for each crystallin protein are shown in Figure 4. All three of them are characterized by the presence of a clear meridional reflection at 4.7 Å and a more diffuse reflection on the equator between 10 and 11 Å. These two reflections are consistent with a β-structure where the β-

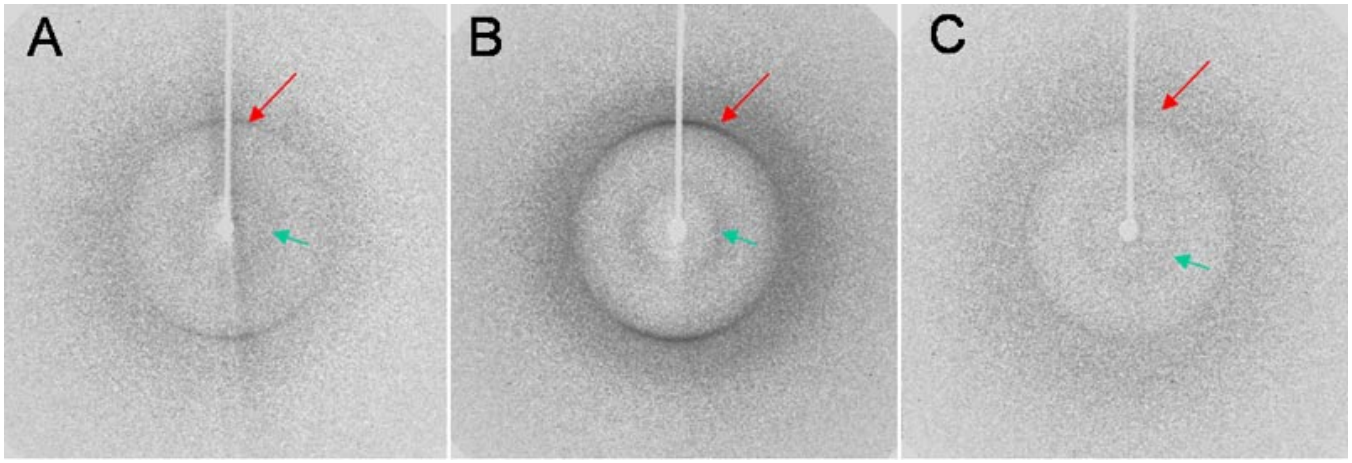

Figure 4. X-ray fiber diffraction from crystallin fibrils. X-ray fiber diffraction patterns recorded for the **A**: HγD-Crys, **B**: HγD-Crys Ctd, and **C**: HγD-Crys Ntd fibrils showing the characteristic features associated with the cross-β amyloid motif: an H-bonding 4.7 Å (long arrow) meridional reflection and an about 10 Å broad reflection (short arrow) on the equator. See experimental procedures for sample preparation.

sheets are spaced by about 10 Å and arranged parallel to the fiber axis with their β-strands lying perpendicular to that direction. The 4.7 Å reflection on the meridian arises from the separation between adjacent strands. The two dominant features constitute the "cross-β" diffraction pattern which along with evidence from electron microscopy and Congo red staining, has come to be considered as diagnostic for amyloid type structures [39,68].

DISCUSSION

The native states of the γ-crystallins are highly soluble and highly stable, showing little or no tendency to polymerize under physiologic conditions. The aggregated states populated during refolding or unfolding in vitro, as with many other protein deposition diseases, are formed of partially unfolded species [17,18,50]. The conformation of the crystallin polypeptide chains that aggregate during refolding at pH7 in vitro are partially unfolded molecules with the COOH-terminal domain native-like and the NH_2-terminal domain disordered. Within the lens such partially unfolded crystallins could be generated by oxidative covalent damage or other environmental stresses. However, the conformations of the aggregated crystallin chains within a mature cataract, or the chains that are precursors to the cataract, have not been characterized.

One aggregated state that is associated with a variety of human diseases is the amyloid fibril [69]. Though mature cataracts do not resemble amyloid plaques, very little is known of the early stage of cataract formation. Meehan and coworkers [50] showed that all three classes of bovine crystallins formed amyloid fibers in vitro, under a particular set of partially denaturing conditions. In mice, a truncated form of γ-crystallin formed inclusions within lens fiber cells that exhibited amyloid character, and the purified truncated protein formed amyloid fibers in vitro upon dilution from the denatured state [51]. These observations led us to examine the propensity of human γD-crystallin to form amyloid fibers. Though low pH environments have not been reported in the lens nucleus, the differentiating epithelial and fiber cells have lysosomes, which presumably maintain the low pH denaturing environment found in other cells.

The results reported here establish that human γD-crystallin forms amyloid fibrils upon incubation at acid pH. Since the full-length protein is composed of two homologous domains, a domain swapping mechanism would provide one model for the polymerization process [70]. However, the isolated COOH-terminal domains also formed amyloid fibers in reasonable yield. This suggests that the Greek key fold itself reorganizes to form the amyloid structure.

Electron microscopy of cataractous lenses in mature onset cataract [71,83,84] do not exhibit the morphological features displayed by amyloid plaques [72]. However, cataracts are generally removed after they have grown to macroscopic dimensions. The early stages have not been identified within the lens. It remains possible that the initiating or nucleating species have a different character than the final bulk aggregate.

Many proteins have been shown to form amyloid fibrils under physiologic or non-physiologic conditions [36,43,45,46]. Thus the formation of amyloid fibrils in vitro does not establish that such reactions might be relevant within the lens. However there is some evidence for the formation of amyloid fibers in both mouse and human lens.

Goldstein and coworkers [73] have reported the presence of amyloid inclusions in cataracts from individuals with Alzheimer disease. The supranuclear cataracts colocalized with enhanced Aβ immunoreactivity and birefringent Congo red staining. In vitro, Aβ was found to promote lens protein aggregation with curvilinear protofibrillar structure. It also has been noted that early-onset cataracts and Alzheimer disease are typical comorbid disorders in adults with Down syndrome [74]. These results raised the possibility that formation of amyloid fibers by crystallins or by other proteins within the lens might stimulate non-amyloid cataract growth.

The lens grows through differentiation of lens epithelial cells into elongated fiber cells. These elongated cells initially have the full spectrum of cell organelles including lysosomes. In fact because of the need to degrade cellular organelles the outer fiber cells at some stage must have very active proteolytic apparatus. The activity of the ubiquitin degradation system has been well documented in lens cells [75]. In the case of amyloid disease due to mutations affecting transthyretin, Kelly and coworkers [41,76] have proposed that the amyloidogenic partially-unfolded intermediate is generated during degradation in the lysosome. Crystallins targeted to lysosomes due to oxidative or photo-oxidative damage might generate amyloidogenic intermediates during breakdown in the lysosomes of outer fiber cells. Since amyloid is very stable under physiologic conditions, these fibers might play a role in nucleating other aggregated states later in the life of the lens.

Recent studies indicate that the relatively disorganized prefibrillar aggregates have greater toxicity to cells than mature fibrils [69,77-81] and consequently it has been suggested that fibril formation could offer, during the early stages of the diseases, a protection against the toxic prefibrillar intermediates [59,69]. In the lens, the damaging effects of cataract, whether or not they include amyloid components, are most likely due to the direct role of large aggregates in scattering light and interfering with image formation. However, disruption of fiber cell organization has been described in cataractous lens [82-84]. Answers to some of these questions will require studying early stages in the formation of cataracts in situ, before they are large enough to interfere with lens transparency.

ACKNOWLEDGEMENTS

This research was supported by NIH grants GM17980 and EYO15834 to J.K., and an Alzheimer Association Award to D.A.K. A.A.R.G., and D.A.K. are grateful to Dr. Andrew Bohm (Dept. of Biochemistry, Tufts University, Boston, MA) for graciously granting access to their X-ray diffraction facility.

REFERENCES

1. Kuszak JR, Clark JI, Cooper KE, Rae JL. Biology of the lens: lens transparency as a function of embryology, anatomy, and physiology. In: Albert DM, Jakobiec FA, Azar DT, Gragoudas ES, editors. Principles and Practice of Ophthalmology, 2nd ed. Philadelphia: W.B.Sauders; 2000. p. 1355-408.
2. Foster A. Cataract—a global perspective: output, outcome and outlay. Eye 1999; 13:449-53.
3. Zigler SJ Jr. Lens Proteins. In: Albert DM, Jakobiec FA, editors. Principles and practice of ophthalmology: basic sciences. Philadelphia: WB Saunders; 1994.
4. Jaenicke R, Slingsby C. Lens crystallins and their microbial homologs: structure, stability, and function. Crit Rev Biochem Mol Biol 2001; 36:435-99.
5. Oyster CW. The human eye: structure and function. Sunderland (MA): Sinauer Associates; 1999.
6. Delaye M, Tardieu A. Short-range order of crystallin proteins accounts for eye lens transparency. Nature 1983; 302:415-7.
7. Boyle D, Takemoto L. Characterization of the alpha-gamma and alpha-beta complex: evidence for an in vivo functional role of alpha-crystallin as a molecular chaperone. Exp Eye Res 1994; 58:9-15.
8. Clark JI, Muchowski PJ. Small heat-shock proteins and their potential role in human disease. Curr Opin Struct Biol 2000; 10:52-9.
9. Cobb BA, Petrash JM. alpha-Crystallin chaperone-like activity and membrane binding in age-related cataracts. Biochemistry 2002; 41:483-90.
10. Horwitz J. Alpha-crystallin can function as a molecular chaperone. Proc Natl Acad Sci U S A 1992; 89:10449-53.
11. Horwitz J. The function of alpha-crystallin in vision. Semin Cell Dev Biol 2000; 11:53-60.
12. MacRae TH. Structure and function of small heat shock/alpha-crystallin proteins: established concepts and emerging ideas. Cell Mol Life Sci 2000; 57:899-913.
13. Aarts HJ, den Dunnen JT, Leunissen J, Lubsen NH, Schoenmakers JG. The gamma-crystallin gene families: sequence and evolutionary patterns. J Mol Evol 1988; 27:163-72.
14. Lampi KJ, Ma Z, Shih M, Shearer TR, Smith JB, Smith DL, David LL. Sequence analysis of betaA3, betaB3, and betaA4 crystallins completes the identification of the major proteins in young human lens. J Biol Chem 1997; 272:2268-75.
15. Basak A, Bateman O, Slingsby C, Pande A, Asherie N, Ogun O, Benedek GB, Pande J. High-resolution X-ray crystal structures of human gammaD crystallin (1.25 A) and the R58H mutant (1.15 A) associated with aculeiform cataract. J Mol Biol 2003; 328:1137-47.
16. Wistow G, Turnell B, Summers L, Slingsby C, Moss D, Miller L, Lindley P, Blundell T. X-ray analysis of the eye lens protein gamma-II crystallin at 1.9 A resolution. J Mol Biol 1983; 170:175-202.
17. Kosinski-Collins MS, Flaugh SL, King J. Probing folding and fluorescence quenching in human gammaD crystallin Greek key domains using triple tryptophan mutant proteins. Protein Sci 2004; 13:2223-35.
18. Flaugh SL, Kosinski-Collins MS, King J. Interdomain side-chain interactions in human gammaD crystallin influencing folding and stability. Protein Sci 2005; 14:2030-43.
19. Hoenders HJ, Bloemendal H. Lens proteins and aging. J Gerontol 1983; 38:278-86.
20. Bova MP, Yaron O, Huang Q, Ding L, Haley DA, Stewart PL, Horwitz J. Mutation R120G in alphaB-crystallin, which is linked to a desmin-related myopathy, results in an irregular structure and defective chaperone-like function. Proc Natl Acad Sci U S A 1999; 96:6137-42.
21. Hejtmancik JF. The genetics of cataract: our vision becomes clearer. Am J Hum Genet 1998; 62:520-5.
22. Heon E, Priston M, Schorderet DF, Billingsley GD, Girard PO, Lubsen N, Munier FL. The gamma-crystallins and human cataracts: a puzzle made clearer. Am J Hum Genet 1999; 65:1261-7.
23. Francis PJ, Berry V, Bhattacharya SS, Moore AT. The genetics of childhood cataract. J Med Genet 2000; 37:481-8.
24. Kmoch S, Brynda J, Asfaw B, Bezouska K, Novak P, Rezacova P, Ondrova L, Filipec M, Sedlacek J, Elleder M. Link between a novel human gammaD-crystallin allele and a unique cataract phenotype explained by protein crystallography. Hum Mol Genet 2000; 9:1779-86.
25. Santhiya ST, Shyam Manohar M, Rawlley D, Vijayalakshmi P, Namperumalsamy P, Gopinath PM, Loster J, Graw J. Novel mutations in the gamma-crystallin genes cause autosomal dominant congenital cataracts. J Med Genet 2002; 39:352-8.
26. Stephan DA, Gillanders E, Vanderveen D, Freas-Lutz D, Wistow G, Baxevanis AD, Robbins CM, VanAuken A, Quesenberry MI, Bailey-Wilson J, Juo SH, Trent JM, Smith L, Brownstein MJ. Progressive juvenile-onset punctate cataracts caused by mutation of the gammaD-crystallin gene. Proc Natl Acad Sci U S A 1999; 96:1008-12.
27. Pande A, Pande J, Asherie N, Lomakin A, Ogun O, King JA, Lubsen NH, Walton D, Benedek GB. Molecular basis of a progressive juvenile-onset hereditary cataract. Proc Natl Acad Sci U S A 2000; 97:1993-8.
28. Pande A, Pande J, Asherie N, Lomakin A, Ogun O, King J, Benedek GB. Crystal cataracts: human genetic cataract caused by protein crystallization. Proc Natl Acad Sci U S A 2001; 98:6116-20.
29. Evans P, Wyatt K, Wistow GJ, Bateman OA, Wallace BA, Slingsby C. The P23T cataract mutation causes loss of solubility of folded gammaD-crystallin. J Mol Biol 2004; 343:435-44.
30. Pande A, Annunziata O, Asherie N, Ogun O, Benedek GB, Pande J. Decrease in protein solubility and cataract formation caused by the Pro23 to Thr mutation in human gamma D-crystallin. Biochemistry 2005; 44:2491-500.
31. Takemoto L, Boyle D. Increased deamidation of asparagine during human senile cataractogenesis. Mol Vis 2000; 6:164-8.
32. Hanson SR, Hasan A, Smith DL, Smith JB. The major in vivo modifications of the human water-insoluble lens crystallins are disulfide bonds, deamidation, methionine oxidation and backbone cleavage. Exp Eye Res 2000; 71:195-207.
33. Stevens A. The contribution of glycation to cataract formation in diabetes. J Am Optom Assoc 1998; 69:519-30.
34. Harding JJ. Cataract, Alzheimer's disease, and other conformational diseases. Curr Opin Ophthalmol 1998; 9:10-3.
35. Mitraki A, King J. Protein folding intermediates and inclusion body formation. Nature Biotechnology 1989; 7:690-9.
36. Dobson CM. Protein misfolding, evolution and disease. Trends Biochem Sci 1999; 24:329-32.
37. Kelly JW. Alternative conformations of amyloidogenic proteins govern their behavior. Curr Opin Struct Biol 1996; 6:11-7.
38. Fink AL. Protein aggregation: folding aggregates, inclusion bodies and amyloid. Fold Des 1998; 3:R9-23.
39. Booth DR, Sunde M, Bellotti V, Robinson CV, Hutchinson WL, Fraser PE, Hawkins PN, Dobson CM, Radford SE, Blake CC, Pepys MB. Instability, unfolding and aggregation of human lysozyme variants underlying amyloid fibrillogenesis. Nature 1997; 385:787-93.

40. Wetzel R. For protein misassembly, it's the "I" decade. Cell 1996; 86:699-702.
41. Kelly JW. The environmental dependency of protein folding best explains prion and amyloid diseases. Proc Natl Acad Sci U S A 1998; 95:930-2.
42. Sipe JD, Cohen AS. Review: history of the amyloid fibril. J Struct Biol 2000; 130:88-98.
43. Bouchard M, Zurdo J, Nettleton EJ, Dobson CM, Robinson CV. Formation of insulin amyloid fibrils followed by FTIR simultaneously with CD and electron microscopy. Protein Sci 2000; 9:1960-7.
44. Chiti F, Webster P, Taddei N, Clark A, Stefani M, Ramponi G, Dobson CM. Designing conditions for in vitro formation of amyloid protofilaments and fibrils. Proc Natl Acad Sci U S A 1999; 96:3590-4.
45. Damaschun G, Damaschun H, Fabian H, Gast K, Krober R, Wieske M, Zirwer D. Conversion of yeast phosphoglycerate kinase into amyloid-like structure. Proteins 2000; 39:204-11.
46. Fandrich M, Fletcher MA, Dobson CM. Amyloid fibrils from muscle myoglobin. Nature 2001; 410:165-6.
47. Guijarro JI, Sunde M, Jones JA, Campbell ID, Dobson CM. Amyloid fibril formation by an SH3 domain. Proc Natl Acad Sci U S A 1998; 95:4224-8.
48. Pertinhez TA, Bouchard M, Tomlinson EJ, Wain R, Ferguson SJ, Dobson CM, Smith LJ. Amyloid fibril formation by a helical cytochrome. FEBS Lett 2001; 495:184-6.
49. Schuler B, Rachel R, Seckler R. Formation of fibrous aggregates from a non-native intermediate: the isolated P22 tailspike beta-helix domain. J Biol Chem 1999; 274:18589-96.
50. Meehan S, Berry Y, Luisi B, Dobson CM, Carver JA, MacPhee CE. Amyloid fibril formation by lens crystallin proteins and its implications for cataract formation. J Biol Chem 2004; 279:3413-9.
51. Sandilands A, Hutcheson AM, Long HA, Prescott AR, Vrensen G, Loster J, Klopp N, Lutz RB, Graw J, Masaki S, Dobson CM, MacPhee CE, Quinlan RA. Altered aggregation properties of mutant gamma-crystallins cause inherited cataract. EMBO J 2002; 21:6005-14.
52. Weinreb O, van Rijk AF, Dovrat A, Bloemendal H. In vitro filament-like formation upon interaction between lens alpha-crystallin and betaL-crystallin promoted by stress. Invest Ophthalmol Vis Sci 2000; 41:3893-7.
53. Kosinski-Collins MS, King J. In vitro unfolding, refolding, and polymerization of human gammaD crystallin, a protein involved in cataract formation. Protein Sci 2003; 12:480-90.
54. Klunk WE, Jacob RF, Mason RP. Quantifying amyloid by congo red spectral shift assay. Methods Enzymol 1999; 309:285-305.
55. Sharma D, Shinchuk LM, Inouye H, Wetzel R, Kirschner DA. Polyglutamine homopolymers having 8-45 residues form slablike beta-crystallite assemblies. Proteins 2005; 61:398-411.
56. Conway KA, Harper JD, Lansbury PT. Accelerated in vitro fibril formation by a mutant alpha-synuclein linked to early-onset Parkinson disease. Nat Med 1998; 4:1318-20.
57. Goldsbury C, Kistler J, Aebi U, Arvinte T, Cooper GJ. Watching amyloid fibrils grow by time-lapse atomic force microscopy. J Mol Biol 1999; 285:33-9.
58. Harper JD, Lieber CM, Lansbury PT Jr. Atomic force microscopic imaging of seeded fibril formation and fibril branching by the Alzheimer's disease amyloid-beta protein. Chem Biol 1997; 4:951-9.
59. Harper JD, Wong SS, Lieber CM, Lansbury PT Jr. Assembly of A beta amyloid protofibrils: an in vitro model for a possible early event in Alzheimer's disease. Biochemistry 1999; 38:8972-80.
60. Ionescu-Zanetti C, Khurana R, Gillespie JR, Petrick JS, Trabachino LC, Minert LJ, Carter SA, Fink AL. Monitoring the assembly of Ig light-chain amyloid fibrils by atomic force microscopy. Proc Natl Acad Sci U S A 1999; 96:13175-9.
61. Lashuel HA, Hartley D, Petre BM, Walz T, Lansbury PT Jr. Neurodegenerative disease: amyloid pores from pathogenic mutations. Nature 2002; 418:291.
62. Lomakin A, Chung DS, Benedek GB, Kirschner DA, Teplow DB. On the nucleation and growth of amyloid beta-protein fibrils: detection of nuclei and quantitation of rate constants. Proc Natl Acad Sci U S A 1996; 93:1125-9.
63. Shen CL, Scott GL, Merchant F, Murphy RM. Light scattering analysis of fibril growth from the amino-terminal fragment beta(1-28) of beta-amyloid peptide. Biophys J 1993; 65:2383-95.
64. Stine WB Jr, Snyder SW, Ladror US, Wade WS, Miller MF, Perun TJ, Holzman TF, Krafft GA. The nanometer-scale structure of amyloid-beta visualized by atomic force microscopy. J Protein Chem 1996; 15:193-203.
65. Walsh DM, Lomakin A, Benedek GB, Condron MM, Teplow DB. Amyloid beta-protein fibrillogenesis. Detection of a protofibrillar intermediate. J Biol Chem 1997; 272:22364-72.
66. Walsh DM, Hartley DM, Kusumoto Y, Fezoui Y, Condron MM, Lomakin A, Benedek GB, Selkoe DJ, Teplow DB. Amyloid beta-protein fibrillogenesis. Structure and biological activity of protofibrillar intermediates. J Biol Chem 1999; 274:25945-52.
67. Zurdo J, Guijarro JI, Dobson CM. Preparation and characterization of purified amyloid fibrils. J Am Chem Soc 2001; 123:8141-2.
68. Geddes AJ, Parker KD, Atkins ED, Beighton E. "Cross-beta" conformation in proteins. J Mol Biol 1968; 32:343-58.
69. Hardy J, Selkoe DJ. The amyloid hypothesis of Alzheimer's disease: progress and problems on the road to therapeutics. Science 2002; 297:353-6. Erratum in: Science 2002; 297:2209.
70. Liu Y, Gotte G, Libonati M, Eisenberg D. A domain-swapped RNase A dimer with implications for amyloid formation. Nat Struct Biol 2001; 8:211-4.
71. Hamai Y, Fukui HN, Kuwabara T. Morphology of hereditary mouse cataract. Exp Eye Res 1974; 18:537-46.
72. Dickson TC, Vickers JC. The morphological phenotype of beta-amyloid plaques and associated neuritic changes in Alzheimer's disease. Neuroscience 2001; 105:99-107.
73. Goldstein LE, Muffat JA, Cherny RA, Moir RD, Ericsson MH, Huang X, Mavros C, Coccia JA, Faget KY, Fitch KA, Masters CL, Tanzi RE, Chylack LT Jr, Bush AI. Cytosolic beta-amyloid deposition and supranuclear cataracts in lenses from people with Alzheimer's disease. Lancet 2003; 361:1258-65.
74. Lowe RF. The eyes in mongolism. Br J Ophthalmol 1949; 33:131-74.
75. Shang F, Taylor A. Function of the ubiquitin proteolytic pathway in the eye. Exp Eye Res 2004; 78:1-14.
76. Colon W, Kelly JW. Partial denaturation of transthyretin is sufficient for amyloid fibril formation in vitro. Biochemistry 1992; 31:8654-60.
77. Bucciantini M, Giannoni E, Chiti F, Baroni F, Formigli L, Zurdo J, Taddei N, Ramponi G, Dobson CM, Stefani M. Inherent toxicity of aggregates implies a common mechanism for protein misfolding diseases. Nature 2002; 416:507-11.
78. Goldberg MS, Lansbury PT Jr. Is there a cause-and-effect relationship between alpha-synuclein fibrillization and Parkinson's disease? Nat Cell Biol 2000; 2:E115-9.
79. Lambert MP, Barlow AK, Chromy BA, Edwards C, Freed R, Liosatos M, Morgan TE, Rozovsky I, Trommer B, Viola KL,

Wals P, Zhang C, Finch CE, Krafft GA, Klein WL. Diffusible, nonfibrillar ligands derived from Abeta1-42 are potent central nervous system neurotoxins. Proc Natl Acad Sci U S A 1998; 95:6448-53.

80. Volles MJ, Lansbury PT Jr. Zeroing in on the pathogenic form of alpha-synuclein and its mechanism of neurotoxicity in Parkinson's disease. Biochemistry 2003; 42:7871-8.
81. Walsh DM, Klyubin I, Fadeeva JV, Cullen WK, Anwyl R, Wolfe MS, Rowan MJ, Selkoe DJ. Naturally secreted oligomers of amyloid beta protein potently inhibit hippocampal long-term potentiation in vivo. Nature 2002; 416:535-9.
82. al-Ghoul KJ, Costello MJ. Morphological changes in human nuclear cataracts of late-onset diabetics. Exp Eye Res 1993; 57:469-86.
83. Al-Ghoul KJ, Lane CW, Taylor VL, Fowler WC, Costello MJ. Distribution and type of morphological damage in human nuclear age-related cataracts. Exp Eye Res 1996; 62:237-51.
84. Gilliland KO, Freel CD, Lane CW, Fowler WC, Costello MJ. Multilamellar bodies as potential scattering particles in human age-related nuclear cataracts. Mol Vis 2001; 7:120-30.

The print version of this article was created on 16 Jan 2008. This reflects all typographical corrections and errata to the article through that date. Details of any changes may be found in the online version of the article.